Journal of Korean Association of Crystal Growth
Vol. 9, No. 4 (1999) 402-416

The formation mechanism of grown-in defects in CZ silicon crystals based on thermal gradients measured by thermocouples near growth interfaces

Takao Abe

Shin-Etsu Handotai, Isobe R&D Center Isobe 2-13-1, Annaka, Gunma 379-0196 Japan

(Received June 9, 1999)

Abstract The thermal distributions near the growth interface of 150 mm CZ crystals were measured by three thermocouples installed at the center, middle (half radius) and edge (10 mm from surface) of the crystals. The results show that larger growth rates produced smaller thermal gradients. This contradicts the widely used heat flux balance equation. Using this fact, it is confirmed in CZ crystals that the type of point defects created is determined by the value of the thermal gradient (G) near the interface during growth, as already reported for FZ crystals. Although depending on the growth systems the effective lengths of the thermal gradient for defect generation are varied, we defined the effective length as 10 mm from the interface in this experiment. If the G is roughly smaller than 20C/cm, vacancy rich CZ crystals are produced. If G is larger than 25C/cm, the species of point defects changes dramatically from vacancies to interstitials. The experimental results after detaching FZ and CZ crystals from the melt show that growth interfaces are filled with vacancies. We propose that large G produces shrunk lattice spacing and in order to relax such lattice excess interstitials are necessary. Such interstitials recombine with vacancies which were generated at the growth interface, next occupy interstitial sites and residuals aggregate themselves to make stacking faults and dislocation loops during cooling. The shape of the growth interface is also determined by the distributions of G across the interface. That is, the small G and the large G in the center induce concave and convex interfaces to the melt, respectively.

1. Introduction

Investigations on native point defects in silicon crystals are classified into the following three categories depending on temperature ranges. First is the research by electron paramagnetic resonance (EPR) at cryogenic temperature on the lattice vacancy and the silicon interstitial produced by electron irradiation, which was performed in full detail by Watkins *et al.* [1] in the 1960s. The second category is associated with two phenomena: one is the enhanced and retarded impurity diffusion induced by oxidation and nitridation, and the other is the kick out and dissociative diffusion of metals such as Au, Pt and Zn in the temperature range of 400~1388 C [2]. The third category concerns the secondary defects of point defects produced during growth of crystal from the melting point to 1000 C. These secondary defects form as a result of non-equilibrium phenomena, that is, the crystal growth and successive cooling which are characterized by the occurrence of thermal gradients. Until now measuring procedures or parameters obtained with the first and second investigations might not be utilized in the main process of the grown-in defect formation near the melting point.

When FZ silicon crystals were first grown without dislocations, the layer structure of defects perpendicular to the growth axis [3] and the so-called "Shallow Pits" which are distributed in swirl-like patterns [4] were observed. De Kock [4] first proposed his model that the origin of the shallow pits was agglomerates of vacancies. Then, however, Foell *et al.* [5] found by a direct observation by TEM that their origins are excess interstitials which make interstitial-type dislocation loops. Presently, such defects are named A defects. As a result of this, many researchers proposed their own models [7-13] as shown in Table 1. Foell *et al.* [7] and Petroff *et al.* [8] discussed their ideas which assumed interstitial silicon to be at equilibrium and non-equilibrium, respectively. Van Vechten [9] and Chikawa *et al.* [10] suggested that, the vacancy is predominant at equilibrium. Even in the vacancy predominant model, Chikawa's droplet model does not exclude the occurrence of A defects. The equilibrium model in which vacancy and interstitial concentration are equal at the growth interface is accepted by many researchers. Sirtl [11] described that pair annihilation and creation is kept with the local equilibrium. Hu [12] and de Kock *et al.* [13] proposed that the A defects generate due to the energy differences of recombination

Table 1
Proposed models on the origin of point defects

	$C_I \gg C_V$	$C_I \ll C_V$	$C_I = C_V$
Equilibrum	*1975 Foell et al: Interstitials* [6] 1977 Foell, Goesele Kolbesen: In equilibrium [7]	1973 de Kock: Vacancies [5] 1978 Van vechten: Cavity model [9]	*1965 Plaskett: Microdefects* [3] 1977 Sirtl: Local equilibrium [11] 1977 Hu: Recombination energy [12] *1981 Roksnoer et al.: D Defect* [14] 1982 Voronkov: Thermodiffusion [15] 1985 Tan et al.: Local equilibrium [16] *1990 Ryuta et al.: COP* [17] *1995 Itsumi et al.: Voids* [18] 1994 Habu: Up hill diffusion [20] 1994 Brown: Thermodiffusion [21] 1995 Ammon: Voronkov's parameter [23]
Non-Equilibrium	1976 Petroff/ de Kock: Impurity clustering [8]	1976 Chikawa/ Shirai: *Interstitials by local remelting* [10] 1983 Abe, Harada/ Chikawa: *Thermal cradient (stress)* [26]	1980 de Kock/van de Wijgert [13] 1984 Roksnoer: Carbon [29]

and agglomeration energies between interstitials and vacancies. In 1981, Roksnoer *et al.* [14] reported another type of defects named the D defects, consisting of excess vacancies, and created by growing FZ crystals with extremely large growth rate. Based on this discovery, Voronkov [15] has developed his theory that the species of intrinsic point defects created depends upon whether the ratio of growth rate (v) and thermal gradient (G) near the growth interface is over or under some critical value (Ccrit), that is,

if $v/G < Ccrit$, interstitial is dominant, and
if $v/G > Ccrit$, vacancy is dominant.

Tan *et al.* [16] tried to modify this theory with a new concept of "the local equilibrium", although it was not yet proved experimentally.

In 1990, Ryuta *et al.* [17] found the crystal originated particles (COP) which are the result of the D defects in CZ crystals, by using a particle counter based on light scattering techniques. Successively, Itsumi *et al.* [18] reported that COPs are twinned structures of octahedral voids covered with thin oxide on inside (111) planes. After those two findings, the trials of numerical simulations to explain the generation of the A and D defects were started by many researchers such as Wijaranakula [19], Habu *et al.* [20] and Brown *et al.* [21], who postulate almost equal concentrations of interstitials and vacancies at the growth interface. They calculated the flux of point defects using the gradient of chemical potentials but the parameters used very widely. Habu *et al.* [20] postulated that both species of point defects at the growth interface are controlled by the G and the v but characterized by uphill diffusion [22] of vacancies. His conclusion is opposite to that of Voronkov, who stated, that if v is large enough, vacancies are predominant and uphill diffusion is negligible.

On the other hand, as it is experimentally known that the dominant species outside and inside of R-OSF is interstitial silicon and vacancy, respectively, Ammon *et al.* [23] and Hourai *et al.* [24] determined the value of v/G on the R-OSF to be 0.13 $mm^2/min \cdot K$ [23]. and 0.22 $mm^2/min \cdot C$ [24], respectively. The former used the commercially available finite element codes FEMAG [25] for the global heat transfer analysis and the latter calculated the temperature distribution in the crystals by ABAQUS [24]. However, the present author and his coworkers measured the temperature

distributions near the growth interface of growing FZ crystal surfaces by a two color thermometer [26]. The results clearly showed that larger v values induce smaller G values. From this result we have proposed that the generation of point defects only depends on G near the growth interface, but not v explicitly which just contributes to change G and to agglomeration of these defects during cooling.

In this paper, we first discuss three points based on the G values actually measured on growing CZ crystals: first is the traditional balance equation used for the computer simulation, second is the meaning of Voronkov's theory and third is the equilibrium model of point defects at the growth interface. In the latter, the species at the growth interface and the effects of thermal gradient on the formation of point defects based on our experimental results are shown and finally the G model of secondary defects formation is described.

2. Experiments

As schematically shown in Fig. 1, two previously grown dislocation-free crystals of lengths of 250 mm and 350 mm with 150 mm in diameter having a conical shoulder but not a conical tail were prepared for measuring temperature distributions during crystal growth. Thermocouples were installed at the flat tail end. To avoid the radiation effects and to measure the temperatures in the crystal interior, three thermocouples at the center, middle (half radius) and edge (10 mm from edge) positions were inserted into the crystals. The diameter of the thermocouples is 1 mm and the outer diameter of their quartz cover is 5 mm. The test crystals were supported by multiple tungsten wires as if real crystals were growing. The weight of melted silicon was adjusted depending on the test crystal length to simulate an initial silicon melt weight of 40 kg. The test crystal was first melted to 10 mm from the tail end of the crystal by dipping a few mm into the melt at a time and waiting for melting to occur, achieving an average melting speed of 0.7 mm/min. Finally, the crystal growth was started, with a growth rate of 1.2 mm/min but no rotation. When the length of the newly grown crystal reached 210 mm from the remelted position, the temperature measurement was halted and the remelting with the above average melting speed was done again to the point 10 mm over the thermocouple positions. In the same manner, the temperature measurements were done for the other three

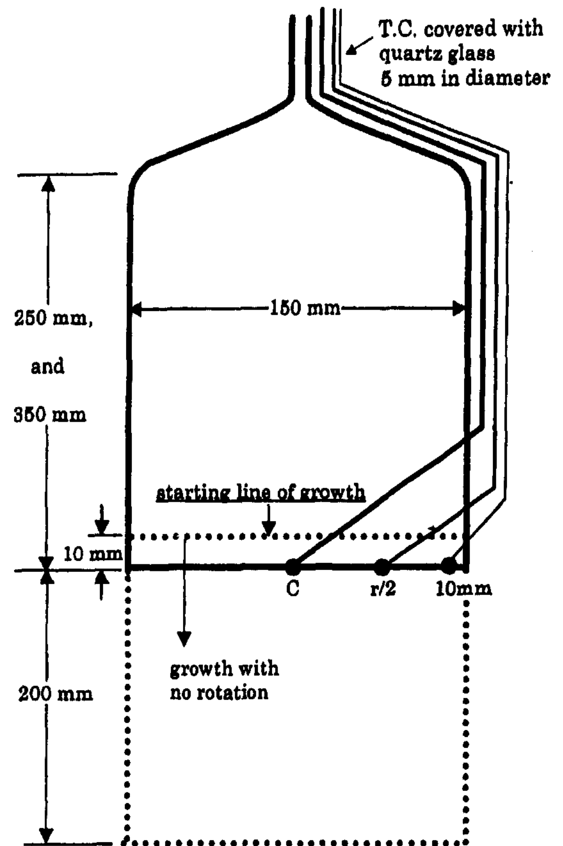

Fig. 1. Schematic of test crystals installed with three thermocouples at the end surface.

cases of growth rates; 1.0 mm/min, 0.6 mm/min and 0.3 mm/min. The temperature distributions of other test crystals of 350 mm in length were also measured by the same manner. A standard CZ puller was used, but was equipped with a hot zone which cools crystals strongly, in order to observe the crystal length effects on G.

3. Results

Figure 2 shows, for four different growth rates, the temperature distributions recorded at the center, middle and edge thermocouple positions in the 250 mm crystal. However, all these profiles are intentionally adjusted to normalize the melting temperature to 1412C because they showed lower temperatures than 1412C at the growth interface. Actual position of the thermocouples may include a few mm errors around the 0 mm position in Fig. 2. Since it is known from

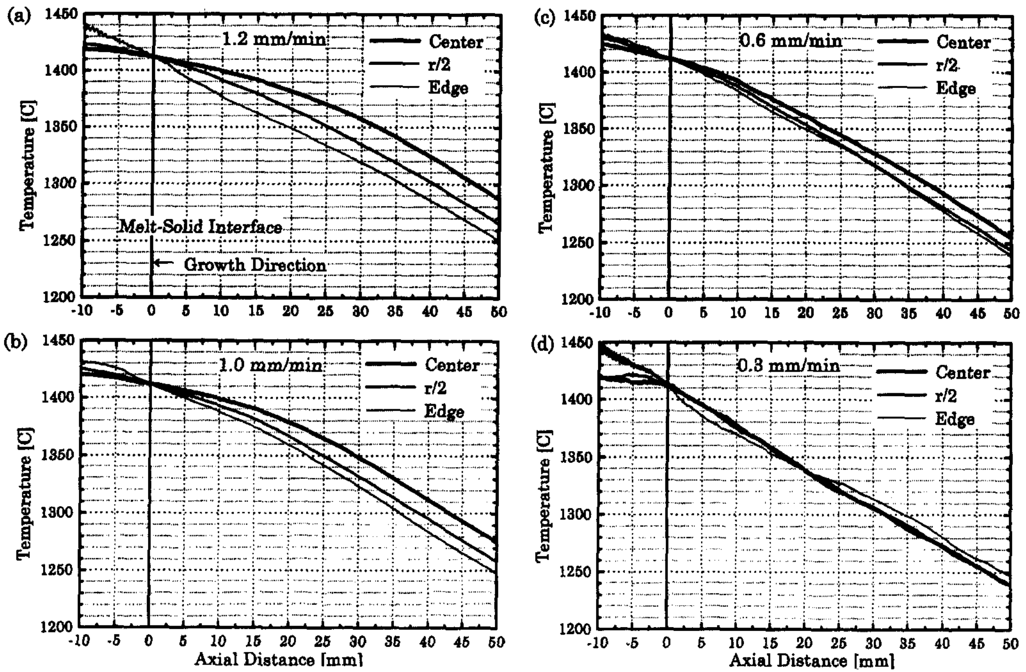

Fig. 2. Axial temperature distributions of 250 mm crystals for four different growth rates using three thermocouples. 1.2 mm/min (a), 1.0 mm/min (b), 0.6 mm/min (c) and 0.3 mm/min (d).

other experiments that the growth interface height with growth rate are postulated as concave to the melt as shown in Table 2, the thermocouple positions passing through the interface are also adjusted in Fig. 2 according to Table 2. In the experiments on the stopping of growth of FZ crystal [26] and the lowering growth rate of CZ crystals [27], secondary defects consisting of interstitials were observed in both crystals, and the effective region for defect generation as measured from the growth interface were several to several tens of millimeters depending on FZ or CZ growth. In this paper, as we defined the effective length as 10 mm from growth interface, the axial temperature gradient G is

$$G = (T_{int} - T_{10})C/cm \quad (1)$$

Table 2
Postulated interface height (concave)

growth rate (mm/min)	center (mm)	middle (r/2) (mm)	edge surface (mm)
1.2	6	5	0
1.0	5	4	0
0.6	3	2	0
0.3	1.5	1	0

The G at the center is the smallest and the G at the edge is the largest in the case of 1.2 mm/min growth rate as shown in Fig. 2 (a). On the other hand, in the case of 0.3 mm/min growth rate the G values in all three positions are almost equal as shown in Fig. 2 (d). The temperature distributions shown in Fig. 2 can be transferred to the isotherms as shown in Fig. 3, if we postulate an axial symmetry of temperature distribution. When v is large, the temperature in the center is higher than that at the edge. On the other hand, when the v is small, a uniform temperature distribution in the cross section of the crystals is obtained. Concerning the interface height in Table 2, it can be said that our supposition is reasonable for Fig. 2 and Fig. 3 based on the following considerations. The smallest G in the center of the crystal with 1.2 mm/min growth rate causes the deepest concave shape due to the weakest heat transfer. If, however, the rotation rate of the seed crystal is large enough, for example 30 rpm, the concave shape is more exaggerated because of ascending forced convection of melt. On the other hand, the large G in the center means the effective heat conduction in the core region leads to a convex shape. It is concluded that the interface shapes are mainly determined by the distributions of G near

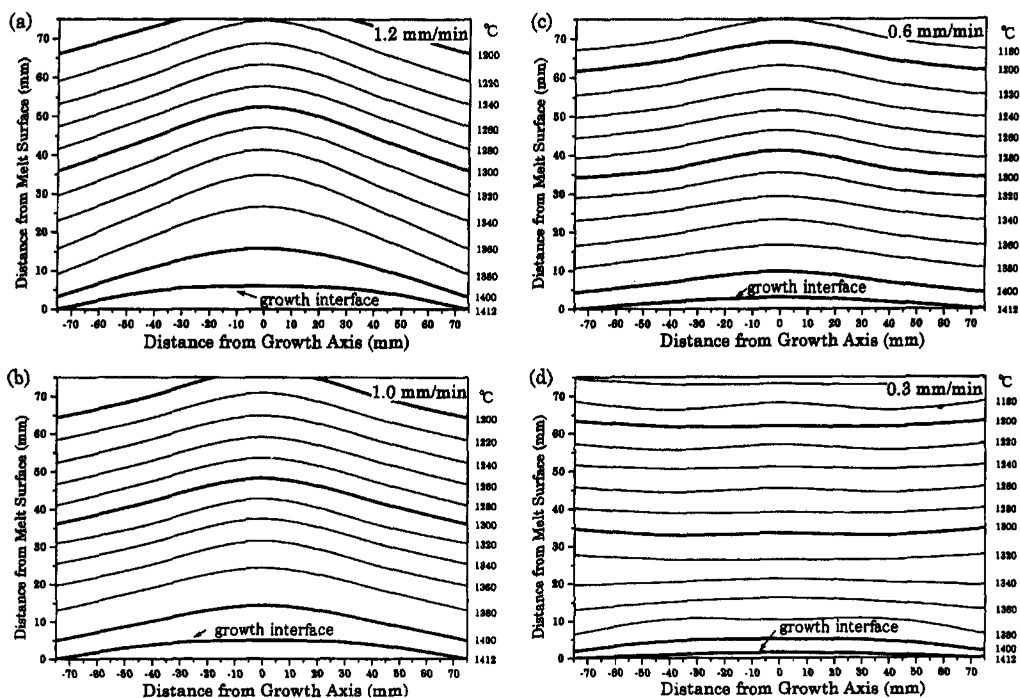

Fig. 3. Isotherms near growth interfaces obtained from Fig. 2. 1.2 mm/min (a), 1.0 mm/min (b), 0.6 mm/min (c) and 0.3 mm/min (d).

the growth interface.

The axial temperature distributions for each thermocouple position as it depends on the growth rate are collected in Fig. 4. The dependence of G on growth rate which a larger v produces a smaller G is obviously demonstrated in the center and middle positions, but at the edge the difference of G values are small for all growth rates. This means that the surface temperature distribution may be largely determined by the type of hot zone within 1.2 mm/min.

Previously reported papers concerning point defect generation have not mentioned the crystal length effects, although some have discussed the thermal history effects caused by the seed side crystal having a longer thermal history than the tail side crystal. In FZ crystal growing, both G and the thermal history do not vary with crystal length, due to rapid cooling effects. However, in CZ crystal growing, it is anticipated that the crystal length has a direct influence on G because of the large contribution of heat conduction through the crystal interior. So we also measured the temperature distributions of the 350 mm crystal in addition to the 250 mm crystal. The order of G values of the 350 mm crystal on growth rate is the same as that of the 250 mm crystal, although in the region far from the growth interface an anomaly in the temperature distributions is observed in the case of 0.6 mm/min growth rate.

In order to consider the length effect, G values are collected as shown in Fig. 5. It is first concluded that smaller v produces larger G in all positions in both Fig. 5 (a) and (b), independent of crystal length, with an exception in the case of 1.2 mm/min growth rate for the 250 mm crystal. On the other hand, in actual crystal growth melt level is descended, after-heating from a heater increases. As result, the G value at the edge becomes small. So to keep the same G, the v must be lowered. In a comparison of Fig. 5 (a) and (b), it is noted that the cross sectional distribution of G changes with crystal length. The G at the edge is larger than that at the center in Fig. 5 (a), but a flat distribution of G and a larger G at the center are seen in Fig. 5 (b). This is a length effect.

4. Discussions

4.1. Balance equation

The following balance equation is widely used as the

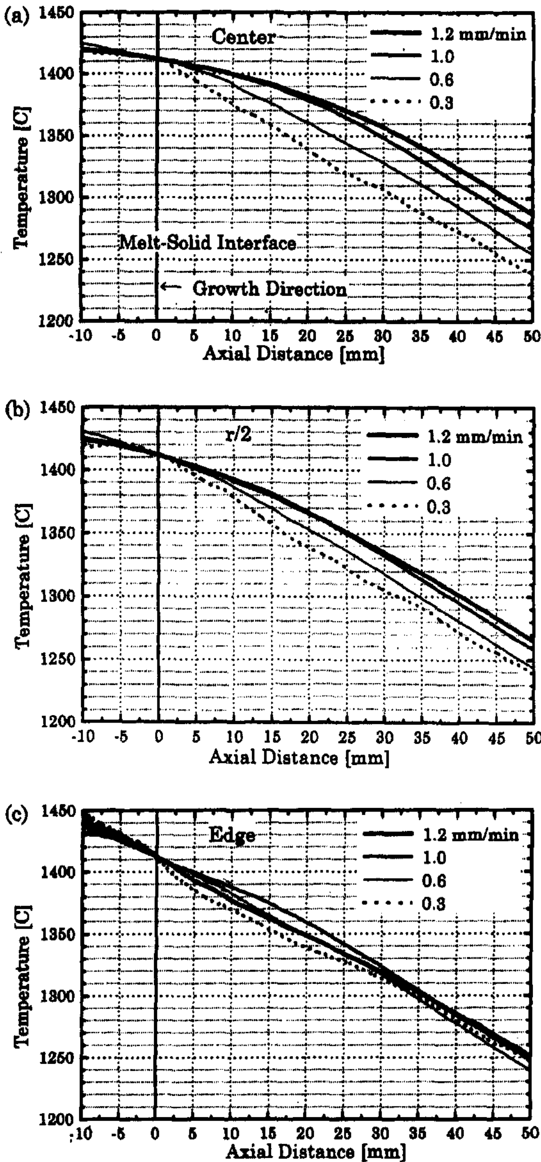

Fig. 4. Axial temperature distributions of 250 mm crystal on each center (a) middle (b) and edge (c) positions obtained from Fig. 2.

boundary condition of heat transfer at a growth interface. If the thermal gradients in solid and liquid at the interface are G_S and G_L then the continuity of heat flux requires:

$$K_S G_S - K_L G_L = L\nu \qquad (2)$$

Where K_S and K_L are the thermal conductivities of solid and liquid and L is the latent heat of solidification per unit volume (ν).

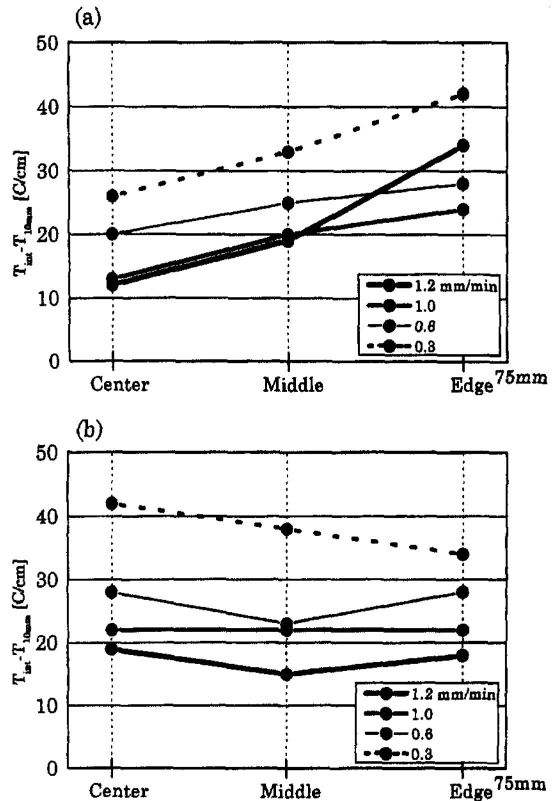

Fig. 5. Temperature gradient G on center, middle and edge depending on growth rates. Crystal length 250 mm (a) and 350 mm (b).

This equation means that when the v becomes large, the G_S must be large. However, independent of crystal length both the results of Fig. 4 and 5 show the opposite behavior near the growth interfaces, that is, the larger v produces the smaller G. In the case of 0.3 mm/min growth rates in Fig. 2 (d) which the G in the melt is smaller than that in the crystal. In addition to this, no effect is seen from the generation of latent heat at the growth interface,

The present results suggest that the above balance equation can not be valid, or useless for silicon with extremely large growth rate compared to that of other materials. Concerning the contradiction of the balance equation with the experimental results, we have to consider the effect of silicon mass transfer in addition to electron and phonon conductions. This means the Gs value becomes small. Moreover, if the v is larger, the sign of the Gs changes to minus. This leads to remelting. As a result, the interface position moves to make a concave interface. On the other hand, when v

is large, the latent heat is transferred by silicon mass. As a results, the temperature distributions continue smoothly through growth interface especially in the center of the crystals as seen in Fig. 4 (a) and (b). When v is small, the discontinuities of temperature distributions at growth interface are shown. The reason is the small contribution of mass transfer but the large contribution of heat conduction through crystals. The small value of the latent heat but the large Gs value bring about the protrude of interface position. So we propose the following equation for the real silicon crystal growth,

$$K_sG_s + L(v) = K_LG_L \qquad (3)$$

but the term of L(v) which is the latent heat transferred to the crystal is a strong function of the v.

4.2. Determination of growth interface shape

In both FZ and CZ crystal growth, it is known that if v and/or the crystal diameter increases, the growth interface shapes tend to concave to the melt. However, the reason for this effect has not been explained yet. From our experimental results, we deduce the formation mechanism of growth interface shape as follows.

In Fig. 4 (d), the temperature distributions near the interface at edge position are almost the same and independence of v but the temperature at the center becomes remarkably higher with increase of v as seen in Fig. 4 (a). It is understood that high temperature material moves with high velocity and the heat conduction is not enough as schematically shown in Fig. 6 (a). However, when the length of the crystal is 350 mm, the heat conduction from the top of crystals is effectively accomplished so that all Gs at the center are larger than those of the 250 mm crystal as shown in Fig. 5 (b). On the other hand, in the case of the small v (0.3 mm/min), the temperatures at both center and edge coincide due to the contribution of heat conduction at the center. In case of the smaller v (0.15 mm/min), G at the center becomes additionally larger. As a result, the interface shape changes from concave to convex as seen in Fig. 6 (b). That is, although the temperature at the edge is constant which is determined by the radiation from a hot zone, the temperature at the center is influenced by the mass transfer from the growth interface and the heat conduction to the upper part of the crystal. In conclusion, the small G and the large G in the center induce concave and convex interfaces to the melt, respectively.

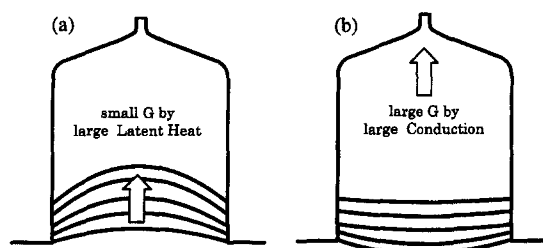

Fig. 6. Schematic of growth interface shape formation. Concave to the melt (a) and convex (b). Surface temp. controlled by radiation but bulk temp. determined by latent heat and conduction.

4.3. Interpretations of previous results [15, 23]

Voronkov's theory [15] is based on the results of Roksnoer's experiment in which extremely large v produced the D defects. It is considered that due to small diameter 23 mm and a pedestal pulling method similar to the FZ process and in which the G near the growth interface is extremely large, reducing the G value by using extremely large v in order to obtain D defects is absolutely necessary. From this results, we can conclude that since the v determines the G in the hot zone, the species of point defects is specified not by the ratio of v over G, but only by G.

Ammon *et al.* [23] recently reported that a critical ratio of v and G, that is $v/G = 1.3\times10^{-3}\ cm^2/min \cdot K$ explains well the R-OSF distribution in the crystals. However, assuming the balance equation they used is not adequate based on results discussed in the previous section, we might interpret their results as follows. The small diameter crystal such as 100 mm itself produces large G, in addition to this the hot zone (HS3) they used produces large G. As the results of it, the only possible procedure to decrease G to obtain $G_{R\text{-}OSF}$ is to use the high growth rate of 1.05 mm/min. As the generation of R-OSF needs a certain thermal gradient such as the $G_{R\text{-}OSB}$ it is understood that this value will be obtained through the controlling of v, because the G is a function of v. From our experimental results in the previous section, it is speculated that the G for R-OSF is roughly in the range of 20~25 C/cm. When a G is <20 C/cm, the R-OSF will not be produced by the change of v even if the relation of $v/G = 0.13\ mm^2/min \cdot K$ is satisfied. Conclusively, the reason why the results by Ammon et al. could explain the distributions of R-OSF is owing to two misunder-

standings: one is the balance equation and another is that the G is not independent of the v. Recently, Puzanov *et al.* [28] presented independently from Voronkov's theory a new computer simulation based on actual microdefect patterns in crystals withdrawal from the melt.

4.4. Species of point defects at growth interface

As mentioned in the introduction section, although researchers had proposed different ideas in the 1980s, equal concentrations of interstitials and vacancies have been postulated in 1990s. On the other hand, detaching techniques from the melt have been utilized for freezing point defects in the vicinity of growth interfaces.

Roksnoer [29] showed that when crystals growing by the pedestal pulling method are detached from the melt and quenched, D defects are always formed near the growth interface as long as the v is over 3.5 mm/min. After the cooling process, D defects convert to A defects below 4.5 mm/min. However, his interpretation on the A defect formation which is different from the present author's idea is as follows. A fraction of carbon atoms in the crystal near the growth interface is incorporated on interstitial lattice sites and then the interaction of interstitial carbon with vacancies is responsible for the change in the dominant type of point defect.

In the CZ process, we detached growing CZ crystals from the melt and cooled them rapidly. A longitudinal specimen cut from such crystal with 75 mm in diameter was annealed at 1000C in dry O_2 for 16 hrs and an x-ray topograph was taken as shown in Fig. 7 (a). The area with white contrast is named as the AOP (anomalous oxygen precipitates) [30] region which is a vacancy rich region. In the crystals without detaching, oxygen precipitation never occurred by a single step annealing at 1000C. The AOP is produced by excess vacancies. Even if the crystal is detached but after that, the crystal cools slowly as if the crystal growth is continued, excess vacancies are faded out and a standard crystal is obtained as shown in Fig. 7 (b). If this crystal goes down again to the detached position which is just on the melt is kept for 30 min. and cooled rapidly, the AOP crystal is reproduced. The length of the AOP from growth interface to the standard area depends on the growth rate. The growth rates of the crystals of Fig. 7 (a) and (b) are 1.0 and 1.2 mm/min, respectively. The length of the AOP region of the crystals with 100 mm in diameter is drastically changed for the small growth rates as seen in Fig. 7 (c) and (d). A smaller v results in a narrower AOP region but a AOP region still exists. However, if

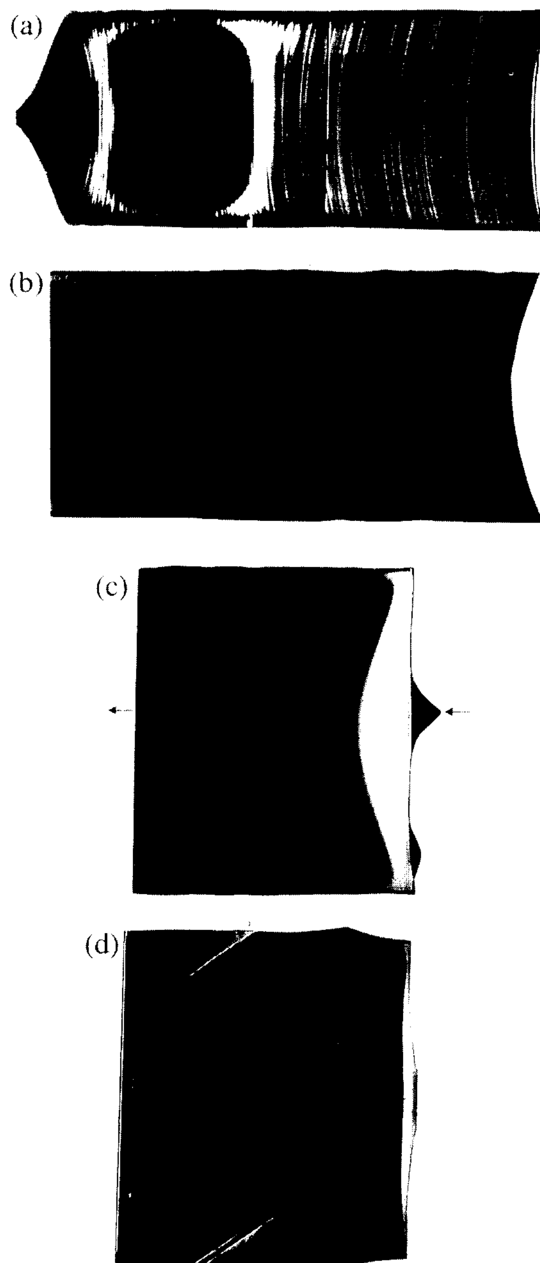

Fig. 7. X-ray topographs of detached crystals annealed with 1000 C, 16 hrs in dry O_2. 75 mm CZ crystal with 1.0 mm/min growth rate (a), slow cooling after detaching (b), 100 mm CZ crystal with 0.47 mm/min (c) and 100 mm CZ crystal with 0.15 mm/min (d).

the crystal is kept to grow with such small v as 0.47 mm/min and 0.15 mm/min without detaching, the whole areas should be converted to the A defect area during cooling due to large G. This is the same phenomenon as mentioned above for Roksnoer's experiments [29]. From this fact, we may conclude that the vicinity of growth interface is always filled with vacancies in both FZ and CZ crystals.

4.5. Interstitials induced by large thermal gradients

4.5.1. FZ crystals

Figure 8 is the x-ray topograph of the crystal with 42 mm in diameter, which stopped to grow for 1, 2 and 4 minutes and then recovered the previous growth rate of 4.0 mm/min. Essentially almost the whole area of the crystal should be filled with D defects as schematically shown in Fig. 9 (a) in all three cases of Fig. 8, but both sides of the stopping position are substituted by the A defects as shown in Figs. 8 (a) and (b). If the cooling rate effect model manages the defect generation, the distribution of the A defect is expected as shown in Fig. 9 (c) because of a cooling rate change only in the already grown crystal.

The following two reactions may explain the phenomenon of Fig. 8. One is the increase of thermal gradient by stopping growth as we showed experimentally

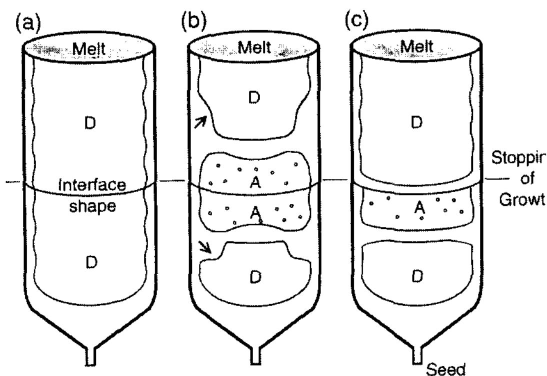

Fig. 9. Schematics for A defect formation. No effect of stopping growth (a), thermal gradient and its inertia effect (b) and cooling effect (c) models.

[25] and the other is the inertia of the large thermal gradient which continues after restarting of growth. The inertia in heat transfer phenomenon is one of the popular features of crystal growth to some extent. As the result, the A defects are generated in both sides of the interface as shown in Fig. 9 (b). The shrinkage of the D defect area marked by arrows is also made by the increasing G but not by the indiffusion of interstitials from surface. The cooling rate effect model like Voronkov's theory can not explain this important phenomena and it is clear that the growth rate itself does

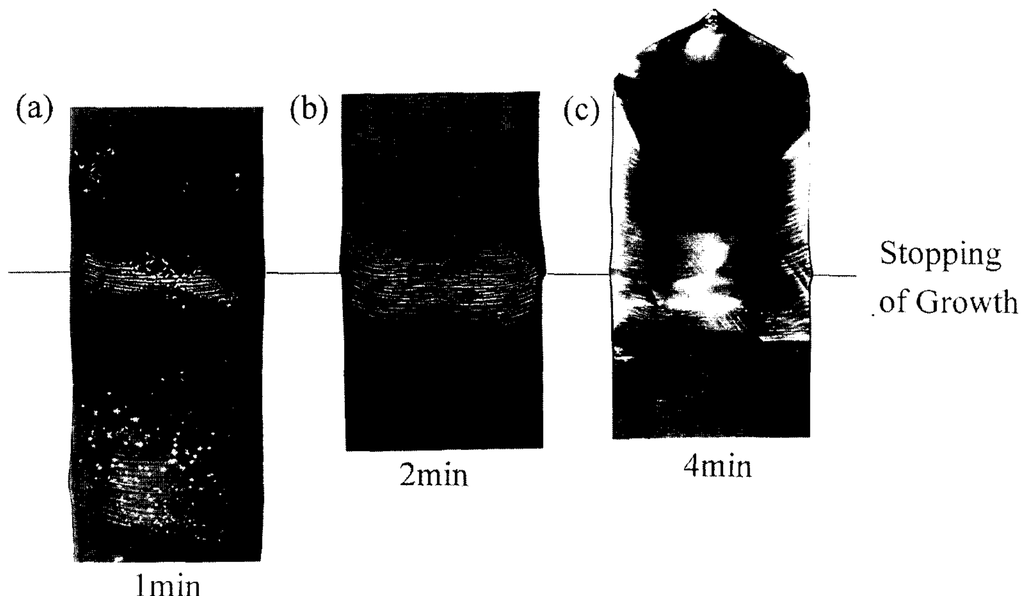

Fig. 8. X-ray topographs of a FZ crystal with stopping growth of first 1 min (a), then 2 min (b) and finally 4 min (c). A defects generate instead of D defects in (a) and (b) but dislocation in (c).

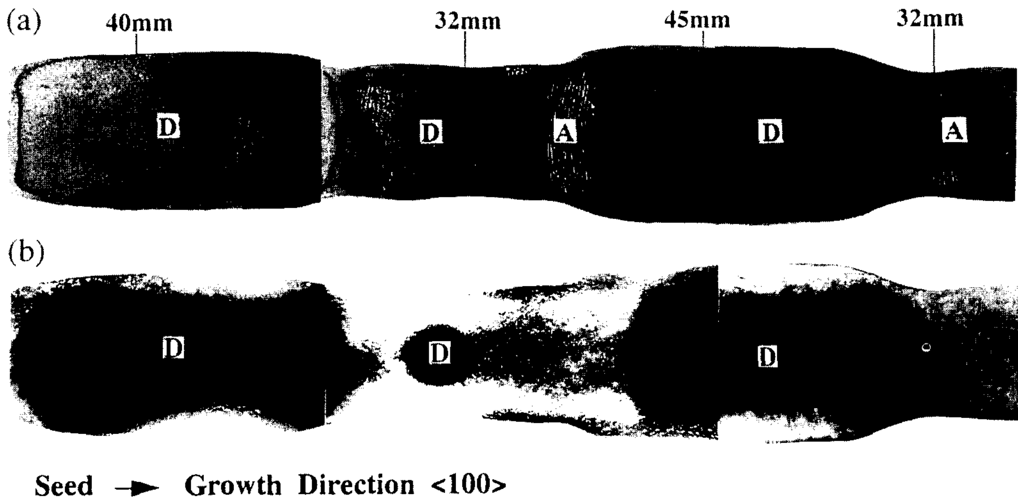

Fig. 10. Diameter effects on a A and D defects in FZ crystals. X-ray topograph after Cu decoration (a) and photograph after depression etching (b).

not relate to generation of point defects because when v = 0, no crystal is grown.

Due to the stopping of growth for 1 and 2 minutes, no dislocations were generated in the crystal but for 4 minutes dislocation free growth converted to dislocated growth. It is understood that the density of interstitial silicon increases with the increase of the stopping period. When the expanding interstitial type dislocation loops reach the growth interface, slip dislocations immediately spread through the whole crystal to relax thermal stress. Such a phenomenon was already reported by de Kock *et al.* [31] and it was confirmed by our results.

Concerning the diameter effects on the thermal gradient, we grew a crystal with constant growth rate of 4.0 mm/min but changed the diameter from 32 mm to 45 mm as seen in Fig. 10 (a) which shows the distribution of the A and D defects. When the diameter is large, due to the small thermal gradient, D defects generate in the center. The reverse is also true. It is noted that A defects distribute near the periphery but D defects always appear in the center. This means that the thermal gradient at the periphery is larger than that of center. Figure 10 (b) shows a photograph of the acid etched surface of the neighbored crystal of Fig. 10 (a). The black contrast is the etching depression [32] area which is caused by reaction of D defects with the acid solution, which corresponds to the D defects in Fig. 10 (a). In conclusion, even at the constant growth rate, the value of the G determines whether A or D defects happen. The diameter effects on the thermal gradient are extremely important but there is little discussion in previous publications.

4.5.2. CZ crystals

In order to confirm the diameter and growth rate effects in (100) CZ crystals, 3 different diameter (50, 100, 200 mm) crystals were grown from one crucible charged with 70 kg in weight. This means that every crystal is grown with exactly same growth condition except diameter. First, a 200 mm crystal was grown with 300 mm in length except top and tail cone parts and the same weight of polycrystal as shown in Table 3 with that of the 200 mm crystal is recharged for next 100 mm crystal. The growth rate is 1.0 mm/min but at 150 mm position immediately decreases to 0.2 mm/min for 30 min, so that the total length of this growth is 6 mm and then recover the previous growth rate. To avoid the abrupt change of diameter due to growth rate change, for example the input heater powers of 78 kwH for 200 mm crystal and 82 kwH for 50 mm crystal increase 14 % and 2.5 % in advance, respectively. The crystal and crucible rotations are 15 and -1.5 rpm, respectively.

The (100) surface specimens were cut longitudinally to the growth direction, chemical-mechanical polished

Table 3
Crystal weights (= recharged weight) of each diameter crystal

Diameter (mm)	200	100	50
Weight (kg)	39.3	8.0	2.5

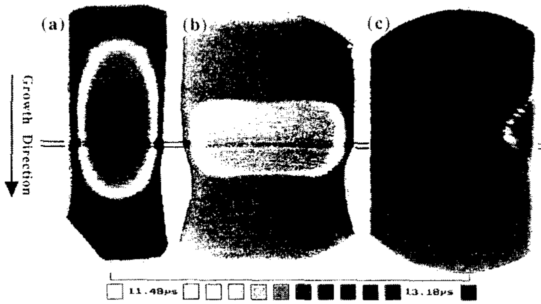

Fig. 11. Wafer lifetime maps of polished surfaces. 50 mm (a), 100 mm (b) and half of 200 mm wafer (c). WLT values are marked by different levels of darkness.

and cleaned by RCA solution. 4 kinds of observation methods are applied for the defect distributions: First is the wafer lifetime as seen in Fig. 11, second is the dark field photograph of Fig. 12, which is taken on the surface etched with Secco's solution for 30 min., third is the microphotographs of Fig. 13 on the surfaces of Fig. 12 and final is the defect densities measured along the growth direction in the center of Fig. 12. The etch pits or defects are two kinds: one is the Secco etch pit (SEP) defect by interstitials type dislocation loops (DLS) and stacking faults (SF) named A defect and the other is the flow pattern (FP) [33] defect related to voids and named D defects or COPs (crystal originated particles).

Concerning the 50 mm crystal, in the lifetime distribution a rugby ball like pattern is seen in Fig. 11 (a). The 0.2 mm/min growth rate region which is 6 mm wide shows relatively high lifetime value but on both sides a rugby ball band which has the lowest lifetime is distributed. This band is the R-OSF band in which

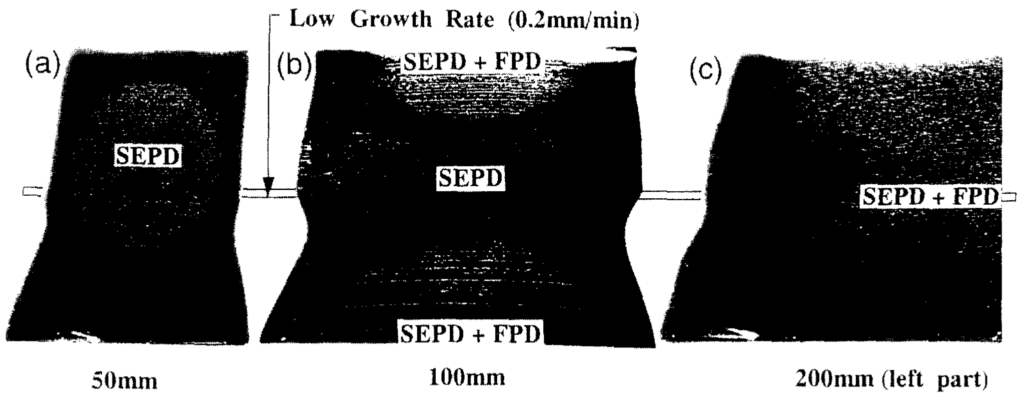

Fig. 12. Darkfield photographs after Secco etching. 50 mm (a), 100 mm (b) and half of 200 mm (c).

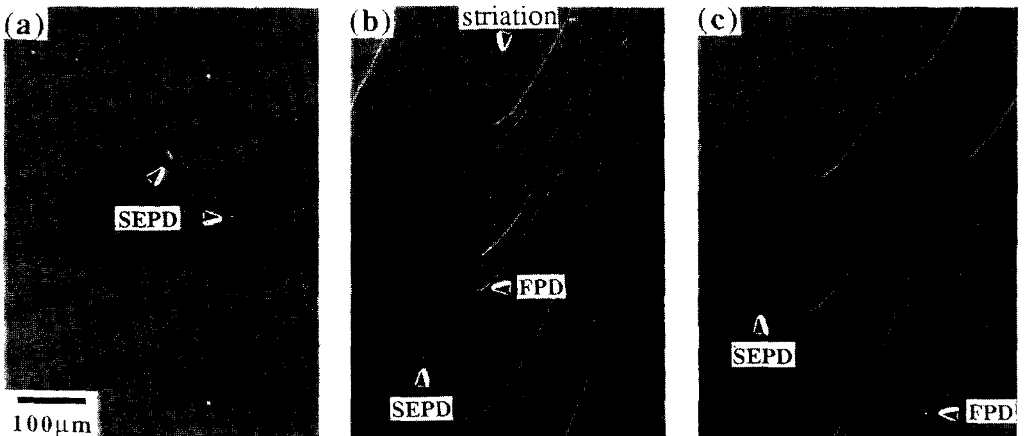

Fig. 13. Microphotographs. (a) is in center part of Fig. 12 (a), (b) is in upper part of Fig. 12 (b) and (c) is in center part of Fig. 12 (c).

only the SF pits are revealed by AFM as seen in Fig. 14 (a). Inside the band coexist both the SF and SE pits as seen in Fig. 13 (a) and Fig. 14 (a) and (b). Outside of the band SE pits are generated. From the above observation, even in the as grown state, stacking faults are already generated during the growth in small diameter crystal with small growth rate. The oxygen concentration of the crystal which is caused by small diameter as seen in Fig. 15 is too low to allow oxygen precipitation. It is reasonable to think that the SF formation is attributed to excess interstitials caused by neither thermal oxidation nor oxygen precipitation

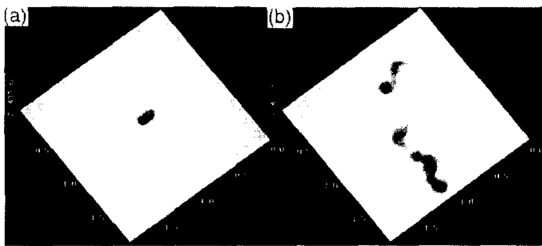

Fig. 14. AFM images on Fig. 12 (a). Stacking fault on SF band (a) and dislocation loops in center (b).

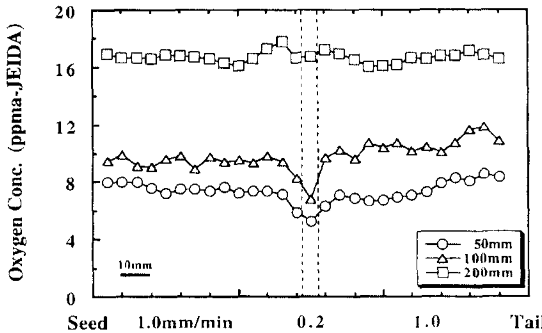

Fig. 15. Oxygen concentration profiles along growth direction in center of Fig. 12.

reaction in the crystal but only by the large G. This means that point defect generation was essentially not connected to oxygen. Figure 16 shows the distributions of SEP density (a) and FP density (b) counted along the growth axis in the centers of Figs. 12 (a), (b) and (c). The SEP defects disperse the whole specimen but in the band the density of SEP defects is higher one order of magnitude as marked as P in Fig. 16 (a). It is also important to note that to FP defects are seen in the whole area Fig. 16 (b).

In case of the 100 mm crystal from the lifetime distribution of Fig. 11 (b), we can recognize that G by the low growth rate is weakened compared to that of the 50 mm crystal as seen in Fig. 11 (a). The rugby ball changes to a cocoon shape which consists of A defects. In the dark field photo of Fig. 11 (b), 3 bright regions are there: the SEP and the FP defects coexist in the outsides of the cocoon region. The core size of the flow pattern pits is very small compared to that of the SE pits but the flow pattern itself scatters light sufficiently to recognize it. D defects in FZ crystals distribute homogeneously but the FP pits in CZ crystals lie along the growth striation as seen in Fig. 13 (b). The FP defects are generated but completely suppressed on the side (cocoon) regions of the small v as seen in Fig. 16 (b). On the contrary the density of the SEP defects markedly increases as seen in Fig. 16 (a). This means that v itself is not a direct parameter for the generation of point defects. A defect-free region with 6mm in width is seen in Fig. 11 (b) which corresponds to the small v region which suggests the defect-free growth reported by Roksnoer *et al.* [11] associated with an extremely small v. It is also speculated that once a defect-free crystal is grown, such a defect free state is maintained, even after large G is applied.

In case of the 200 mm crystal, the influence of the

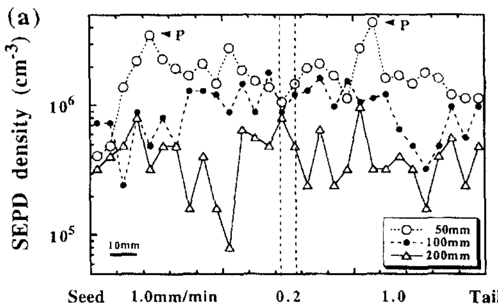

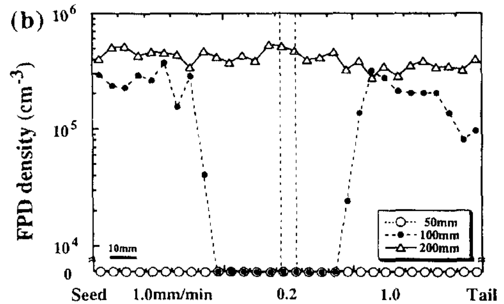

Fig. 16. SEP and FP defect density distributions along growth direction in center of Fig. 12 (a), (b) and (c). SEP defects (a) and FP defects (b).

small v is the smallest but the R-OSF is formed and the FP defect is free in the periphery as seen in Fig. 11 (c) and 12 (c), respectively. The drastic changes of the defect densities are not caused by the small v but the density of the SE pits is lower one order of magnitude than that of the others in Fig. 16 (a) and the maximum density of the FP defects is observed in Fig. 16 (b). This is due to the large heat capacity of large diameter crystal so that G decreases. Because of the increase of G by the small growth rate of 0.2 mm/min, interstitials are generated far from growth interface, and then mixed and recombined between vacancies which generate at growth interface. However, the recombination of interstitials with vacancies is not a complete, so that residual interstitials aggregate to make DLs over 1200 C and then vacancies aggregate to make voids under 1200 C. This is the reason why interstitial and vacancy defects coexist generally in large diameter crystals.

4.6. Proposed mechanism of grown-in defect formation

There are many discussions [7, 8] in which silicon becomes dominant by interstitial rich at the growth interface when the phase transition from melt to solid occurs due to the density change of 10 % in silicon. However, according to the previous section the reality is quite opposite. This can be explained by the new concept [36] that a high density of vacancies in the silicon melt is preserved in the silicon lattice. The reason is as follows. The structure of silicon melt is similar to a type of β-Sn [37]. When β-Sn structure transfers to α-Sn structure (similar to diamond structure), the density of Sn increases by 1.255. The density of the silicon melt should be about 2.889 g/cm^3 but reality is about 2.603/cm^3. It is speculated that silicon melt has to contain a high density of vacancies. As a result, a vacancy rich silicon lattice is formed using this melt.

During the next cooling step, if G is large near the growth interface, the lattice shrinks as schematically shown in Fig. 17 (a). To relax the shrunk lattice and to recover the equilibrium lattice parameter at each temperature, excess interstitials are necessary to expand the lattice as shown in Fig. 17 (a). First, such interstitials are used for recombining with vacancies which were generated at the growth interface, second they occupy interstitial sites and finally in the cooling process but over 1200 C they aggregate to generate the A defects such as SFs and DLs. All these configurations are useful to expand the lattice. In small diameter crystals which have larger G compared to that of large diameter crystals, it is easy to be covered by the A defects. On the other hand, in large diameter crystals, as complete recombination with vacancy is difficult due to small G, the residual vacancies still aggregate by themselves to make the D defects so that both the A and D defects tend to coexist. However, even in 300mm crystals, we can grow crystals containing only the A defects, only the D defects or without both defects by controlling G. Such G values are governed by many parameters but mainly diameter, growth rate and the design of a hot zone.

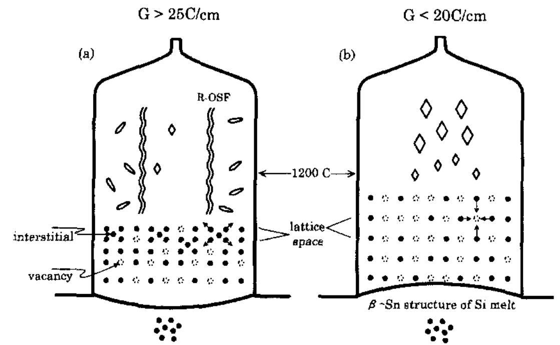

Fig. 17. Proposed model of grown-in defects in CZ crystal. Higher thermal gradient G > 25 C/cm (a) and lower G < 20 C/cm (b).

On the other hand, if there is a mall G near the growth interface, the expanding lattice is hold but to recover the equilibrium lattice parameter a high density of vacancies is necessary to shrink the lattice as seen in Fig. 17 (b). The role of excess vacancies is to obtain compressive stress of the lattice. Under 1200 C, they aggregate to make the D defects.

In our experimental system mentioned in sub-heading of CZ crystals in the previous section, from the wafer life time results of Fig. 11 the region (6 mm) grown with extremely small growth rate of 0.2 mm/min seems to show more complete crystal quality than that of the other region. This region of the crystal may not contain excess vacancies, although the A defects still exist as seen in Fig. 16 (a). The crystals with extremely small growth rate bring about perfect crystals which was also reported by Roksnoer *et al.* [14]. Under 0.2 mm/min range, in-diffusion of interstitials from growth interface to bury vacancies is possible. On the other hand, as we discussed in 4.4, the growth interface is filled with vacancies. Figure 18 shows the profiles of oxygen concentration along the

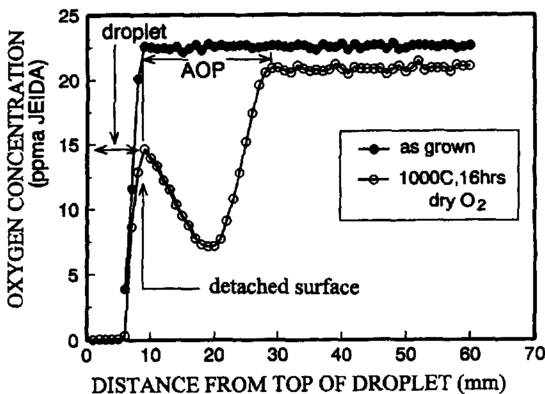

Fig. 18. Profiles of oxygen concentrations along growth direction through a droplet marked by an arrow in Fig. 7 (c).

growth direction through a droplet marked by an arrow in Fig. 7 (c). Solidus circles show the oxygen concentration of the as-detached crystal. In the droplet, the result is under the detection limit of oxygen because during solidification probably within one minute oxygen evaporates. The AOP region which corresponds to the white contrast region in Fig. 7 (c) is enhanced by oxygen precipitation as shown in Fig. 18. However, in the half width of the AOP region near the detached surface, oxygen precipitation is retarded. One can speculate that during cooling, interstitials indiffuse from the surface and recombine with excess vacancies.

In the temperature distributions of growing crystals of these experiments, the G at the periphery is larger than that at the center in the crystals which grow with relatively large v. It is natural that such distributions cause the A defects at the periphery and the D defects at the center. In the boundary of both defects R-OSF bands are formed as seen in Fig. 17 (a).

5. Conclusions

The thermal distributions near the growth interface of 150 mm CZ crystals were measured by three thermocouples installed at the center, middle (half radius) and edge (10 mm from surface) of the crystals. The results show that larger growth rates produced smaller thermal gradients. This contradicts the widely used heat flux balance equation. Using this fact, it is claimed that in CZ crystals the type of point defects created is determined by the value of the thermal gradient (G) near the interface during growth, as already reported for FZ crystals. Although depending on the growth systems, the effective lengths of the thermal gradient for defect generation vary, we defined the effective length as 10 mm from the interface in this experiment. When the G is roughly smaller than 20 C/cm, vacancy rich CZ crystals are produced. While the G is larger than 25 C/cm, the species of point defects changes dramatically from vacancies to interstitials. The experimental results involving FZ and CZ crystals detached from the melt suggest that growth interfaces are filled with vacancies. We propose that large G values produce a shrunken lattice spacing and in order to relax such lattice, excess interstitials are necessary. Such interstitials recombine with vacancies which were generated at the growth interface, next occupy interstitial sites and residuals aggregate themselves to form stacking faults and dislocation loops during cooling. The shape of the growth interface is also determined by the distributions of G across the interface. The small G and the large G value in the center induce concave and convex interfaces to the melt, respectively.

Acknowledgments

The author thanks M. Iida and M. Kimura of SEH Isobe R&D Center for measuring the temperature distributions of growing crystals and Prof. N. Inoue (Osaka Pref. Univ.) and Prof. K. Wada (MIT) for valuable discussions in this work. The author also wishes to thank Prof. G. Mueller (Univ. Erlangen) for criticism on measurements and Prof. U. Goesele (MPI/ Halle) for preparation of the manuscript.

References

[1] G. Watkins, Defects and Diffusion in Silicon Processing, ed. T. Diaz, de la Rubia, S. Coffa, P.A. Stalk and C.S. Rafferty, p. 139 MRS Symp. Vol. 469 Warrendale, PA (1997).
[2] H. Bracht, E.E. Haller, K. Eberl, M. Cardona, and R. Clark-Phelps. Mat. Res. Soc. Symp. Proc. 527 (1998) 335.
[3] T.S. Plaskett, Trans. AIME, 233 (1965) 809.
[4] T. Abe, T. Samizo and S. Maruyama, Jpn. J. Appl. Phys. 5 (1966) 458.
[5] A.J.R. de Kock, Appl. Phys. Lett. 16 (1970) 100.
[6] H. Foell and B.O. Kolbesen, Appl. Phys. 8 (1975) 319.
[7] H. Foell, U. Goesele and B.O. Kolbesen, Semiconductor Silicon 1977, ed. H.R. Huff and E. Sirtl

(Electrochem. Soc., Princeton, 1977) p. 565.
[8] P.M. Petroff and A.J.R. de Kock, J. Cryst. Growth 30 (1975) 117.
[9] J.A. Van Vechten, Phys. Rev. B17 (1978) 3179.
[10] J. Chikawa and S. Shirai, Jpn. J. Appl. Phys. 18, Suppl. 18-1 (1979) 153.
[11] E. Sirtl, Semiconductor Silicon 1977, ed. H.R. Huff and E. Sirtl (Electrochem. Soc., Princeton, 1977) p. 4.
[12] S.M. Hu, J. Vacuum Sci. & Technol. 14 (1977) 17.
[13] A.J.R. de Kock and W.M. Van de Wijgert, J. Cryst. Growth 49 (1980) 718.
[14] P.J. Roksnoer and M.M.B. Van Den Moom, J. Cryst. Growth 53 (1981) 563.
[15] V.V. Voronkov, J. Cryst. Growth 59 (1982) 625.
[16] T.Y. Tan and U. Goesele, J. Appl. Phys. A 37 (1985) 1.
[17] J. Ryuta, E. Morita, T. Tanaka and Y. Shimanuki, Jpn. J. Appl. Phys. 29 (1990) L1947.
[18] M. Itsumi, H. Akiya and T. Ueki, J. Appl. Phys. 78 (1995) 5984.
[19] E. Wijaranakula, J. Electrochem. Soc. 139 (1992) 604.
[20] R. Habu, I. Yunoke, T. Saito and A. Tomiura, Jpn. J. Appl. Phys. 32 (1993) 1740.
[21] R.A. Brown, d. Maroudas and T. Sinno, J. Cryst. Growth 137 (1994) 12.
[22] W.W. Webb, J. Appl. Phys. 33 (1962) 1961.
[23] W.V. Ammon, E. Dornberger, H. Oelkrug and H. Weidner, J. Cryst. Growth 151, No. 3/4 (1995) 273.
[24] M. Hourai, E. Kajita, T. Nagashima, H. Fujiwara, S. Ueno, S. Sadamitsu, S. Miki and T. Shigematsu, Materials Science Forum Vols. 196-201 (1995) p. 1713.
[25] F. Dupret, P. Nicodeme, Y. Ryckmans, P. Wouters and M.J. Crochet, Int. J. Heat Mass Transfer 33 (1990) 1849.
[26] T. Abe, H. Harada and J. Chikawa, Physica 116B (1983) 139.
[27] T. Abe and K. Hagimoto, Solid State Phenomena 47-48 (1996) 107.
[28] N. Puzanov, A. Eidenson and D. Puzanov. Abstract of the ICCG 12/ICVGE 10, July 1998, Jerusalem p. 342.
[29] P.J. Roksnoer, J. Cryst. Growth 68 (1984) 596.
[30] H. Harada, T. Abe and J. Chikawa, Semiconductor Silicon 1986, ed. H.R. Huff, T. Abe and B.O. Kolbesen (Electrochem. Soc. Penningston, 1986) p. 76.
[31] A.J.R. de Kock, P.J. Roksnoer and P.G.T. Boron, J. Cryst. Growth 30 (1975) 279.
[32] W. Keller and A. Muehbouer, Inst. Phys. Conf. Ser. No. 23 (The Inst. of Physics, London and Bristal 1974) p. 538.
[33] H. Yamagishi, I. Fusegawa, N. Fujimaki and M. Katayama, Semicond. Sci. Technol. 7 A135 (1992).
[34] W. Lin and M. Stavola, J. Electrochem. Soc. 132 (1985) 1412.
[35] E. Iino, K. Takano, I. Fusegawa and H. Yamagishi, Semiconductor Silicon 1994, ed. H.R. Huff, W. Bergholz and K Sumino, (Electrochem. Soc. Pennington 1994) p. 148.
[36] M. Suezawa (private communication).
[37] Y. Waseda and K. Suzuki, Z. Phys. B20 (1975) 339.